

Southern Ocean albedo, inter-hemispheric energy transports and the double ITCZ: global impacts of biases in a coupled model

Matt Hawcroft¹  · Jim M. Haywood^{1,2} · Mat Collins¹ · Andy Jones² · Anthony C. Jones¹ · Graeme Stephens³

Received: 16 February 2016 / Accepted: 20 May 2016 / Published online: 3 June 2016
© The Author(s) 2016. This article is published with open access at Springerlink.com

Abstract A causal link has been invoked between inter-hemispheric albedo, cross-equatorial energy transport and the double-Intertropical Convergence Zone (ITCZ) bias in climate models. Southern Ocean cloud biases are a major determinant of inter-hemispheric albedo biases in many models, including HadGEM2-ES, a fully coupled model with a dynamical ocean. In this study, targeted albedo corrections are applied in the Southern Ocean to explore the dynamical response to artificially reducing these biases. The Southern Hemisphere jet increases in strength in response to the increased tropical-extratropical temperature gradient, with increased energy transport into the mid-latitudes in the atmosphere, but no improvement is observed in the double-ITCZ bias or atmospheric cross-equatorial energy transport, a finding which supports other recent work. The majority of the adjustment in energy transport in the tropics is achieved in the ocean, with the response further limited to the Pacific Ocean. As a result, the frequently argued teleconnection between the Southern Ocean and tropical precipitation biases is muted. Further experiments in which tropical longwave biases are also reduced do not yield improvement in the representation of the tropical atmosphere. These results suggest that the dramatic improvements in tropical precipitation that have been shown in previous studies may be a function of the lack of dynamical ocean and/or the simplified hemispheric albedo bias corrections applied in that work. It further suggests

that efforts to correct the double ITCZ problem in coupled models that focus on large-scale energetic controls will prove fruitless without improvements in the representation of atmospheric processes.

Keywords Climate models · Albedo · Southern Ocean · ITCZ · Energy transport

1 Introduction

Many global climate models (GCMs) exhibit considerable biases in the representation of the observed hemispheric albedo symmetry (Voigt et al. 2014b; Loeb et al. 2015), leading to associated biases in cross-equatorial energy transport. A typical—and frequently significant—contribution to this hemispheric albedo bias is from the Southern Ocean, where many models fail to reproduce the observed cloud distribution around extratropical cyclones, leading to excessive shortwave absorption in this region (Bodas-Salcedo et al. 2012, 2014; Williams et al. 2013). Biases in cross-equatorial energy transport (Loeb et al. 2015) and the Southern Ocean (Hwang and Frierson 2013) have both been invoked to explain the double Intertropical Convergence Zone (ITCZ) bias which is a feature of many GCMs. The mechanism for this relationship is that a warmer Southern Hemisphere atmosphere increases northward atmospheric energy transport at the equator and leads to a southward shift in the location of maximum tropical precipitation associated with the ITCZ. These biases have persisted in many generations of GCMs (Hwang and Frierson 2013; Zhang et al. 2015).

One model which exhibits biases across these metrics which are typical of the current generation of GCMs is HadGEM2-ES, the coupled atmosphere–ocean Earth

✉ Matt Hawcroft
m.hawcroft@exeter.ac.uk

¹ College of Engineering, Mathematics and Physical Sciences, University of Exeter, Exeter, UK

² Met Office Hadley Centre, Exeter, UK

³ Jet Propulsion Laboratory, Pasadena, CA, USA

system model of the Met Office Hadley Centre (Collins et al. 2011). The model has been shown to accurately reproduce observed surface temperatures (Collins et al. 2011) but exhibits biases in the Southern Ocean (Bodas-Salcedo et al. 2012), hemispheric albedo, cross-equatorial energy transport and the ITCZ (Haywood et al. 2016). The global pattern of top-of-atmosphere (TOA) shortwave and longwave radiation biases in HadGEM2-ES is comparable to many current GCMs (Li et al. 2013), with substantial underestimates of TOA outgoing shortwave radiation in the Southern Ocean and associated overestimates of TOA outgoing longwave radiation. In the tropics, biases in the TOA longwave are related to cloud biases, with too much outgoing longwave where monsoon cloud cover is underestimated and errors associated with the location of the ITCZ and South Pacific Convergence Zone (SPCZ).

Previous work has shown that perturbing cross-equatorial energy transport, including through changes to the energy budget of the extratropics, influences the location of the ITCZ in simplified frameworks, such as aquaplanet (e.g. Voigt et al. 2014a, b) or slab ocean experiments (e.g. Chiang and Bitz 2005; Kang et al. 2008; Frierson and Hwang 2012; Cvijanovic and Chiang 2013). The ITCZ moves in the opposite direction of the atmospheric energy flux anomaly. A southward cross-equatorial energy transport anomaly induces a northward moisture flux anomaly which pushes the ITCZ further north, and vice versa. For these purposes, the energy and moisture fluxes at the equator can be considered proxies for the upper and lower branch of the southern branch of the Hadley circulation, thereby modulating the ITCZ location (see Hwang and Frierson 2013, Figure 4, for a schematic of this mechanism). The use of slab ocean configurations has been justified on the basis it provides a closed surface energy budget. However, to explore the full dynamical response of the climate system to any perturbations in the inter-hemispheric energy budget a coupled model framework is required.

The recent work of Kay et al. (2016) is of particular relevance to the present study. The aim of Kay et al. was to assess the global climate impact of reducing shortwave biases in the Southern Ocean in the CESM-CAM5 model, with adjustments made in the tropics to maintain the global TOA energy balance. These bias corrections were achieved through modifying cloud properties. They found that meridional energy transport changes in the tropics were dominated by adjustments in ocean energy transport, particularly through changes in the Pacific Ocean circulation. Atmospheric energy transport in the tropics were significantly smaller such that the ITCZ did not respond to the extratropical forcing and the double ITCZ bias in the model persisted. In a slab ocean experiment, which included their shortwave bias corrections, they found a large improvement in the ITCZ as the required adjustments in meridional

energy transport had to be achieved in the atmosphere. CESM-CAM5 exhibits similar Southern Ocean and tropical shortwave biases to HadGEM2-ES.

In another study of relevance, Deser et al. (2015), investigating responses to Arctic sea ice loss in the CCSM4 model, found very different responses in coupled and slab simulations. The atmospheric response to this high latitude perturbation was confined to north of 30°N in slab experiments but had global impacts in a coupled model framework, including a shift in the ITCZ. Both these studies underline the importance of a dynamic ocean to understanding the response to albedo/energy budget anomalies.

Haywood et al. (2016) have shown a significant improvement in the representation of tropical precipitation in HadGEM2-ES in a series of simplified experiments where hemispheric albedo is equilibrated through perturbing the Southern Hemisphere radiation budget. Haywood et al. used a coupled model framework and simplified, hemisphere wide, perturbations to the Southern Hemisphere radiation balance through stratospheric aerosol, cloud brightness and surface reflectance adjustments. The focus of that study was on the tropical response and the simplified, hemisphere wide, nature of the applied forcings are such that a near step change in the top-of-atmosphere energy budget is induced at the equator. This study expands upon those results by applying smooth corrections to both shortwave and longwave budgets in a series of experiments which target the location of these biases, such as the Southern Ocean, rather than applying a consistent perturbation across the whole Southern Hemisphere. Through targeted corrections to the energy budget the dynamical response can be more readily interpreted with respect to the observed climate. As in Haywood et al. (2016), the aim of this study is not to identify the processes within the model which are responsible for the biases (see e.g. Bodas-Salcedo et al. 2014), but to examine the potential for an improved representation of the climate of the model if these biases are addressed. In addition to building upon Haywood et al. (2016), this study is highly complementary to that of Kay et al. (2016), since the present work investigates the impact of reducing the same, Southern Ocean, albedo biases that were a focus of Kay et al. in an entirely independent climate model with a different experimental design. The present study then goes on to consider the further impact of reducing longwave biases, which neither Haywood et al. (2016) or Kay et al. (2016) considered.

In Sect. 2 the model and experimental set-up is described, along with the observational datasets used to constrain the model. In Sect. 3 the results of the experiments are discussed, first by evaluating the response of the model where only the shortwave biases are corrected and then considering the model's response when both shortwave and longwave biases are reduced. The findings,

limitations and implications of the study are summarised in Sect. 4.

2 Data and methods

2.1 HadGEM2-ES climate model

HadGEM2-ES (Collins et al. 2011) is a fully coupled atmosphere–ocean climate model developed by the Met Office Hadley Centre. The atmospheric component has 38 levels extending to 40 km, with a horizontal resolution of $1.25^\circ \times 1.875^\circ$ in latitude and longitude, respectively, equivalent to a surface resolution of about 200 km \times 140 km at the Equator, reducing to 120 km \times 140 km at 55° latitude. ES refers to the Earth System version, which includes coupling to a tropospheric chemistry scheme, the terrestrial carbon cycle and an ocean biogeochemistry scheme. The oceanic component has 40 unevenly spaced vertical levels and a latitude–longitude grid with a zonal resolution of 1° globally and meridional resolution of 1° poleward of 30°N/S , which increases smoothly from 1° at 30°N/S to $1/3^\circ$ at the equator. Aspects of the response of HadGEM2-ES's ocean to external forcing have been shown to be realistic (Menary et al. 2013; Menary and Scaife 2014) and the model's representation of certain Southern Ocean processes compares favourably to other models (e.g. Heuzé et al. 2013; Meijers 2014).

2.2 Experimental design

Haywood et al. (2016) performed a series of experiments where the albedo in the Southern Hemisphere of HadGEM2-ES was increased through adjustments to stratospheric aerosol optical depth, ocean albedo and cloud droplet number concentration. A significant improvement in cross-equatorial atmospheric energy transport, and a related improvement in tropical precipitation, was found in all experiments. The results of the Haywood et al. experiments were qualitatively similar to each other even though the energy budget perturbations were applied differently in each case. In the present study, we apply a latitudinally varying forcing which targets the source regions of the bias, such as the Southern Ocean. In this framework, perturbing stratospheric aerosol or cloud droplet number concentration is not practical. Ocean albedo is therefore perturbed in order to adjust the TOA shortwave radiation budget towards observations (the 'SWex' simulations) and is justified based on the similarity of Haywood et al.'s results to different forcings. As discussed in Sects. 3 and 4, the results of this study bear remarkable similarity to those of Kay et al. (2016), where cloud properties were adjusted, lending further support to this idealised approach. Zonally

Table 1 Hemispheric average albedo and the difference between Southern (SH) and Northern (NH) Hemisphere in CERES, CLIM and the four members of the SWex ensemble

	Average albedo		
	SH	NH	SH–NH
CERES	0.2912	0.2917	0.0005
HIST	0.2889	0.3003	−0.0114
SWex1	0.2931	0.2941	−0.0010
SWex2	0.2958	0.2957	0.0001
SWex3	0.2969	0.2965	0.0004
SWex4	0.2999	0.2934	0.0065

uniform perturbations to direct and diffuse ocean albedo are applied to counterbalance global annual mean biases in TOA albedo when compared to CERES observations, as further discussed in Sect. 3. These experiments only have a direct impact on the shortwave budget of the model, with any changes in the longwave controlled by the dynamical response to the shortwave perturbation. The experiments are designed to reduce and reverse the hemispheric albedo bias in the model—with the Southern Hemisphere progressively brightened as the Northern Hemisphere reflectivity is reduced (Table 1)—which has implications for cross-equatorial energy transport. Decreasing albedo in the Southern Hemisphere relative to the Northern Hemisphere is expected to lead to southward energy transport anomalies at the equator. The partitioning of these energy transport anomalies between the atmosphere and ocean then governs the dynamical response in the tropical atmosphere.

The total (ocean plus atmosphere) meridional energy transport is a function of the net TOA energy flux (shortwave and longwave). The SWex experiments only target the shortwave biases in the model. If these experiments do not lead to significant improvements in the atmospheric circulation, residual energy transport biases will be retained. A second set of experiments is therefore performed where, in addition to the ocean albedo adjustments, longwave biases in the model are reduced through inserting a climatology of cirrus-like clouds in the tropics (the 'SWLWex' simulations), centred on 12°S and 5°N , since an absence of high tropical clouds is a source of the longwave bias in the model (see, for example, Jiang et al. 2012). We design these clouds to be radiatively active only in the longwave and they do not interact with the cloud physics, convection scheme or interactive aerosol scheme, other than through any modifications the heating from these clouds may have on the climate. We emphasise that these experiments are not designed to be realistic, but build on the SWex ensemble with the purpose of assessing the model response when the TOA energy budget is further constrained towards observations, through both direct shortwave and longwave

adjustments, forcing the total meridional energy transport in the model towards the observed climate system.

The experiments are compared to a present day simulation (CLIM) which is integrated using the CMIP5 (Taylor et al. 2012) historical emissions pathway from 1860. The experiments use the same emissions pathway with the experimental simulations initialised from the CLIM experiment in 1978. Two decades of data (1980–1999) are shown here, though a subset of experiments were run for 100 years. The conclusions of the work were not affected by the longer integration period and the circulation changes analysed here are observed within the first few years of the simulations (not shown). Kay et al. (2016) found a similar, fast response in their simulations with no material change in the model response after 200 years of simulation time. Given the timescale on which the Atlantic meridional overturning circulation has been observed to adjust to perturbations in other studies using HadGEM2-ES (Menary et al. 2013; Menary and Scaife 2014), 100 years is more than sufficient to confirm the full dynamical response of the model to forcing has been achieved in the first two decades.

2.3 Diagnostics

Total meridional energy transports (TET) in the model are calculated across each latitude band (ϕ) by integrating the TOA radiative fluxes (R_T) from one pole to the other, discounting the total atmospheric heat tendency ($\frac{\partial A_E}{\partial t}$) and total ocean heat tendency ($\frac{\partial O_E}{\partial t}$), which may be non-zero in the transient experimental framework employed here:

$$TET(\phi) = \int_{-\pi/2}^{\phi} \int_0^{2\pi} \left(R_T - \frac{\partial A_E}{\partial t} - \frac{\partial O_E}{\partial t} \right) a^2 \cos\phi \, d\lambda \, d\phi, \quad (1)$$

where λ is longitude and a is the radius of the earth. Ocean energy transport (OET) is calculated explicitly in the model and the atmospheric transport (AET) is the difference between TET and OET.

Meridional latent energy and dry energy transports are calculated as the vertical integrals of the meridional fluxes of latent energy and, for the dry energy, the sum of dry static energy and kinetic energy (as for NCAR (2014)).

During the period from 2000 to 2013, when observations have been available from the Clouds and the Earth's Radiant Energy System (CERES, Wielicki et al. 1996) project, the net total (shortwave and longwave) TOA imbalance in radiation is approximately 0.6 Wm^{-2} , with an uncertainty of $\pm 0.4 \text{ Wm}^{-2}$ (at the 90 % confidence level) in the CERES observations (Loeb et al. 2012b; Stephens and L'Ecuyer 2015). The experiments here are all designed to achieve a top-of-atmosphere energy budget which is closed to within these limits. In Haywood et al. (2016), the experiments were not designed to maintain total TOA energy balance and

quasi-uniform albedo adjustments were applied across the Southern Hemisphere. In Haywood et al. (2016), although improvements in tropical precipitation over land were found, cold biases were induced across most areas because of the TOA imbalance. This work builds on that study by eliminating both the cooling effect and the near step change in the TOA radiation budget at the equator whilst continuing to investigate the impact of hemispheric albedo adjustments.

2.4 Observational datasets

TOA and surface radiative fluxes are obtained from the CERES (Wielicki et al. 1996) Energy Balanced and Filled (EBAF) Ed2.8 product (Loeb et al. 2009, 2012a; Kato et al. 2013). The climatology used here is March 2003–February 2013, the longest period available at the time of this study. CERES derives flux estimates from broadband instruments situated on the orbiting *Aqua* and *Terra* satellites in addition to 3-hourly estimates from geostationary satellites which are cross-calibrated using Moderate Resolution Imaging Spectroradiometer (MODIS) data (Doelling et al. 2013).

Meridional energy transports are calculated using CERES TOA fluxes (R_T), combined with total atmospheric heat tendency ($\frac{\partial A_E}{\partial t}$) and divergence estimates ($\nabla \cdot F_A$) from the ERA-Interim (Dee et al. 2011) dataset (see Loeb et al. 2015), which are obtained from NCAR (2014), and total ocean heat tendencies ($\frac{\partial O_E}{\partial t}$) from the ORAS4 dataset (Balmaseda et al. 2013). The ORAS4 data is annual and is from 2003–2012 to maximally overlap with the CERES and ERAI data. The atmospheric energy transports (AET) are calculated by integrating the atmospheric divergence of energy ($\nabla \cdot F_A$) from one pole to the other. Ocean energy transport (OET) across each latitude band (ϕ) is derived as follows:

$$OET(\phi) = \int_{-\pi/2}^{\phi} \int_0^{2\pi} \left(R_T - \nabla \cdot F_A - \frac{\partial A_E}{\partial t} - \frac{\partial O_E}{\partial t} \right) a^2 \cos\phi \, d\lambda \, d\phi, \quad (2)$$

and TET across each latitude band is the sum of AET and OET. The $\frac{\partial A_E}{\partial t}$ and $\frac{\partial O_E}{\partial t}$ terms are very small (less than ± 0.005 and $\pm 0.011 \text{ PW}$, respectively, at any given latitude) relative to the transport terms, so the uncertainty in their absolute magnitudes (see, for example, Palmer et al. 2015) has no material impact on the differences in energy transport seen between the model and observations. They are taken into account to appropriately apportion the net TOA energy imbalance of $\sim 0.6 \text{ Wm}^{-2}$ between atmosphere and ocean during the analysis period—if they are not taken into account, then a residual transport term remains as an artefact in the OET (and TET) at the pole which the OET is integrated towards. Meridional latent energy and dry energy transports are from the ERA-Interim dataset and are also obtained from NCAR (2014).

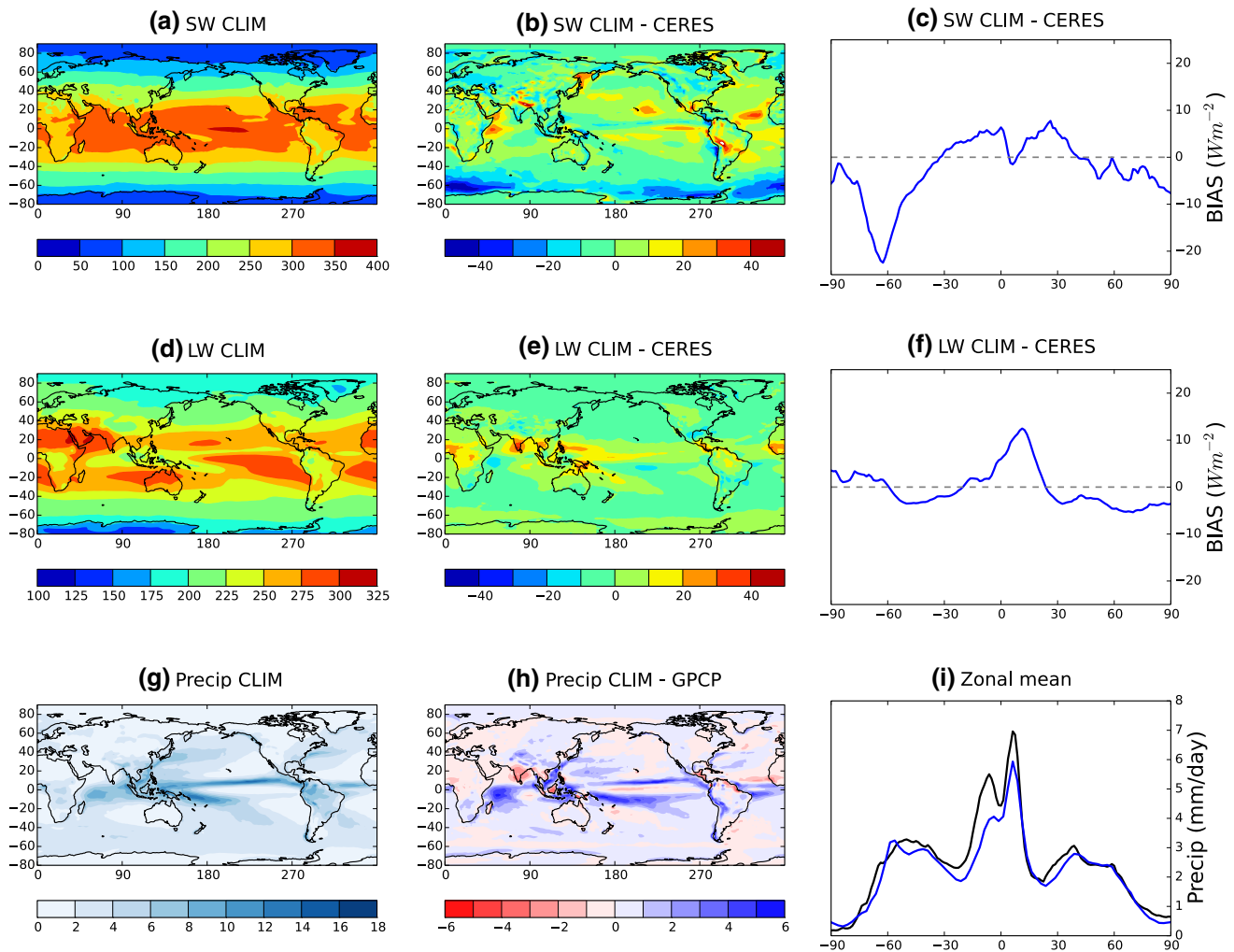


Fig. 1 Top of atmosphere net shortwave (a–c) and longwave (d–f) radiation (W m^{-2}) and precipitation (g–i) mm day^{-1}) showing the model climatology (CLIM, a, d, g) with the model bias (b, e, h) and

the zonal mean bias compared against CERES (c, f upwards as *positive*) and zonal mean precipitation compared against GPCP (i model in black and GPCP in blue)

Precipitation estimates are obtained from the Global Precipitation Climatology Project (GPCP) version 2.2 data (Adler et al. 2003) over the period 1979–1998. GPCPv2.2 is a global, $2.5^\circ \times 2.5^\circ$ gridded, monthly dataset that combines multiple satellite estimates and rain gauge data to produce precipitation estimates. The satellite estimates are tuned using monthly gauge observations. Bias error in the climatological zonal mean precipitation in the tropics is estimated to be less than 0.2 mm day^{-1} (see Adler et al. 2012, Figure 4).

3 Results

3.1 Shortwave bias reduction

In Fig. 1, TOA shortwave and longwave fluxes are shown from the CLIM simulation, with their biases relative to

CERES. A clear, large underestimate of outgoing shortwave radiation can be seen in the Southern Ocean, which is typical of the current generation of GCMs (Li et al. 2013, Figure 11; Kay et al. 2016) and are associated with too little cloud cover around extratropical cyclones (Bodas-Salcedo et al. 2012). This bias peaks around 70°S , where the zonal mean bias is stronger than 20 W m^{-2} (Fig. 1c). Across the tropics, the zonal mean outgoing shortwave is overestimated in HadGEM2-ES, though this is a function of a more complex pattern of local under/overestimation.

In the longwave, the most significant biases are in the tropics where outgoing longwave radiation (OLR) is overestimated (Fig. 1e). This is typically associated with areas that have too little precipitation, such as over India and West Africa. SST errors do not dominate tropical longwave biases, with OLR errors generally associated with biases in cloud location (not shown). The zonal mean OLR bias

over the land is twice that of the ocean where the total bias peaks around 12°N (not shown). The double ITCZ bias in the model is clear in Fig. 1i and is primarily a function of the extended South Pacific Convergence Zone (e.g. Van Der Wiel et al. 2015a, b) in the model and excessive precipitation in the South East Indian Ocean (Fig. 1h). The underestimate of precipitation along the equator in the Pacific is related to the cold tongue being extended too far west in the model (not shown) when compared to observations. These are both typical biases for models of this generation (Dai 2006; Zhang et al. 2015).

To investigate the impact of reducing shortwave biases in the model, the ocean albedo is adjusted in the SWex experiments, as shown in Fig. 2a, up to a maximum value of the ocean albedo equalling 1. Typical values of ocean albedo in the model are 0.06–0.09, with 0.07–0.08 in the Southern Ocean, such that the perturbed ocean albedo is unlikely to reach this physical limit in the experiments. The variations in forcing across the ensemble of experiments are designed to elucidate the impact of a reduction and reversal of the inter-hemispheric albedo bias in the model on the representation of cross-equatorial energy transport and tropical precipitation when that forcing is applied in a targeted fashion. Southern Hemisphere albedo is progressively increased in the experiments (see Table 1) with a reduction in Northern Hemisphere average albedo which both alters the inter-hemispheric albedo and also maintains global TOA energy balance.

Total cross-equatorial energy transport is forced to change through these adjustments and the atmospheric response is determined by the partitioning of these changes between atmosphere and ocean—in a slab ocean experiment the total response would be confined to the atmosphere (see e.g. Kang et al. 2008; Frierson and Hwang 2012; Cvijanovic and Chiang 2013). Total northward cross-equatorial energy transport in CLIM is 0.85PW and this is reduced to 0.77/0.64/0.67/0.52 PW in the four SWex simulations. The CERES estimate is 0.25 PW, with a likely uncertainty range of ± 0.1 PW (Stephens et al. 2016). The improvement in cross-equatorial energy transport biases is partial, even in the experiment where the inter-hemispheric albedo bias is reversed and is related to the fact the total TOA net radiation (Fig. 2d) does not improve dramatically due to the persistence of longwave biases. This issue is further discussed below.

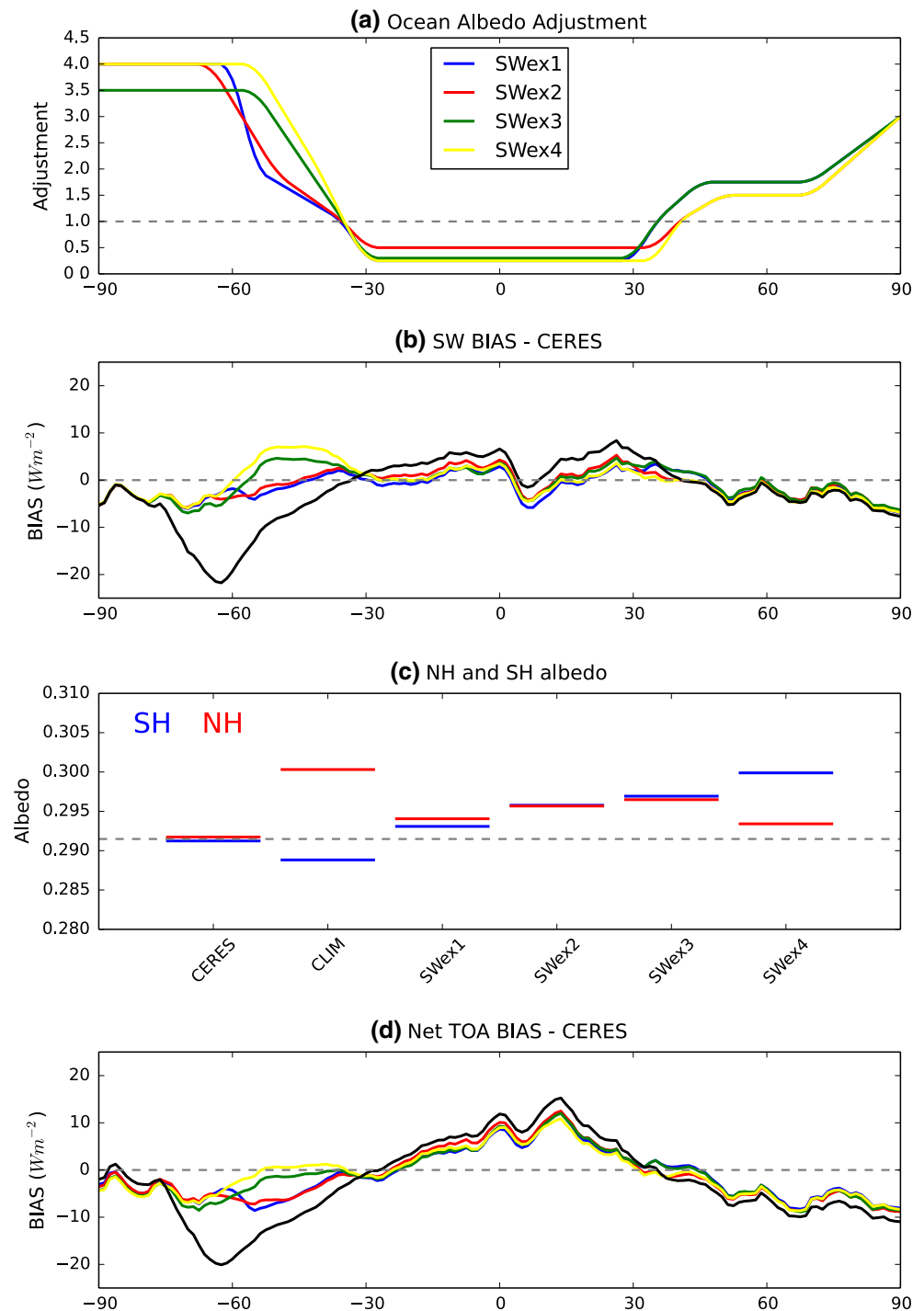
In Fig. 2b the zonal mean shortwave biases in CLIM and SWex are shown, compared to CERES, demonstrating the uniform improvement in the TOA shortwave budget in the SWex simulations. The details differ across the ensemble due to the specific design of each experiment—which sought to reduce local shortwave biases, change inter-hemispheric biases and maintain TOA energy balance—though are qualitatively similar. The ensemble of experiments all reduce the Southern Ocean and tropical TOA biases, with

the hemispheric albedo bias (Table 1; Fig. 2c) reduced then reversed.

Figure 3 shows the dynamical response in the SWex ensemble. As the albedo of the Southern Ocean is increased, less energy is absorbed by the climate system in the extratropics and the climate in this region cools. Simultaneously, the albedo of the tropics is reduced, such that more energy is absorbed by the climate system in the tropics, leading to warming. The net effect of this cooling of the extratropics and warming of the tropics is an increase in poleward energy transport. There is an increase in the strength of the jet via thermal wind balance (centred on 200 hPa) in the Southern Hemisphere in all experiments (Fig. 3b–e). In the Northern Hemisphere, small increases in jet strength are also observed, though they are less substantial due to the smaller perturbation applied when compared to the Southern Hemisphere. Given the spectrum of changes in albedo and cross-equatorial energy transport which are applied in HadGEM2-ES, it might be expected (Haywood et al. 2013, 2016) that the tropical precipitation response in the SWex simulations would diverge, with the response increasing as the perturbation to inter-hemispheric albedo increases. Figure 3g–j shows that this is not the case.

In all experiments, there is an increase in tropical precipitation in the Southern Hemisphere relative to CLIM, making the pre-existing double ITCZ bias worse (see Fig. 4a, b). It is of note that the changes in tropical precipitation in the experiments are largely confined to the Pacific, with the South Pacific Convergence Zone (SPCZ) expanding and smaller reductions in precipitation in the central Pacific north of the equator (around 220°E, 5°N). This bias has a seasonal signature, with the SPCZ expanding during austral summer (DJF), when maximum insolation is in the Southern Hemisphere, with a smaller zonal precipitation bias during boreal summer (JJA). A comparison of zonal mean precipitation over land and ocean points in each of these seasons (Fig. 5) provides further insight into the nature of these biases. Precipitation is too intense over the ocean in both summer and winter seasons in both hemispheres and there is a better representation of precipitation over land. Zonal mean precipitation biases over land are less than 1 mm day^{-1} at almost all latitudes, whereas zonal mean precipitation biases over the ocean can exceed 3 mm day^{-1} in the tropics. The ocean precipitation biases between 5 and 15°S in DJF are primarily a signature of the SPCZ biases. In JJA, the bias in oceanic precipitation centred on 10°N is associated with the ITCZ being too intense in the Pacific, Atlantic and Indian Oceans. In neither season are the zonal precipitation biases improved between the CLIM and SWex simulations, suggesting that the perturbations to the energy budget have had relatively little impact on tropical atmospheric circulation, other than in the Pacific south of the equator.

Fig. 2 Shortwave forcing applied and response obtained in the experiments: **a** the zonally uniform adjustment (multiplication of existing albedo, up to a maximum albedo of 1) to the ocean albedo applied to the model, **b** the zonal mean bias (W m^{-2} , upwards as *positive*) in the *top* of atmosphere net shortwave radiation in the CLIM (*black*) simulation and the four SWex experiments as a result of the forcing applied in **a** compared to CERES, **c** the mean albedo in the Northern and Southern Hemisphere (NH/SH) in CERES, CLIM and SWex, **d** the zonal mean bias (W m^{-2} , upwards as *positive*) in the *top* of atmosphere net radiation (shortwave and longwave) in CLIM and SWex compared to CERES



The differential response in the atmospheric circulation in the tropics and extratropics can be reconciled with reference to the changes in meridional energy transport from the CLIM simulation to SWex. Figure 6 shows the total (TET), ocean (OET) and atmosphere (AET) energy transport in CLIM, observations (from CERES, ERAI and ORAS4) and SWex. In Fig. 6a it can be seen that too little energy (TET) is being transported into the Southern Hemisphere extratropics

in CLIM when compared to observations. This bias is partitioned between both AET and OET, with both fluxes too low in the Southern Hemisphere mid-latitudes. This bias is also evident in the Northern Hemisphere transport terms. The SWex ensemble all reduce these biases (Fig. 6b) though the partitioning of the response is particularly interesting.

In the tropics, the increase in Southern Hemisphere TET is largely achieved in the ocean (Fig. 6b). In the

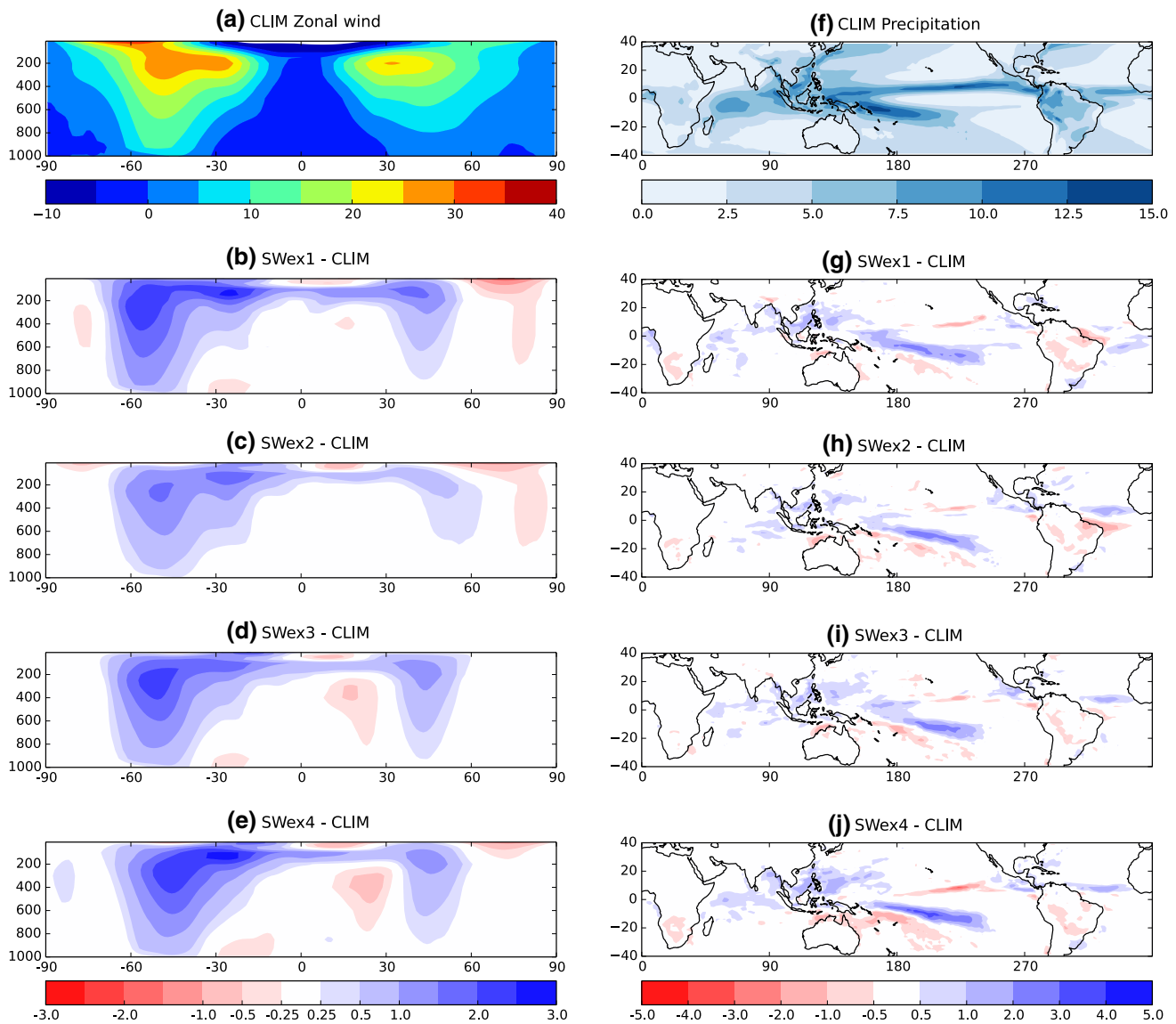
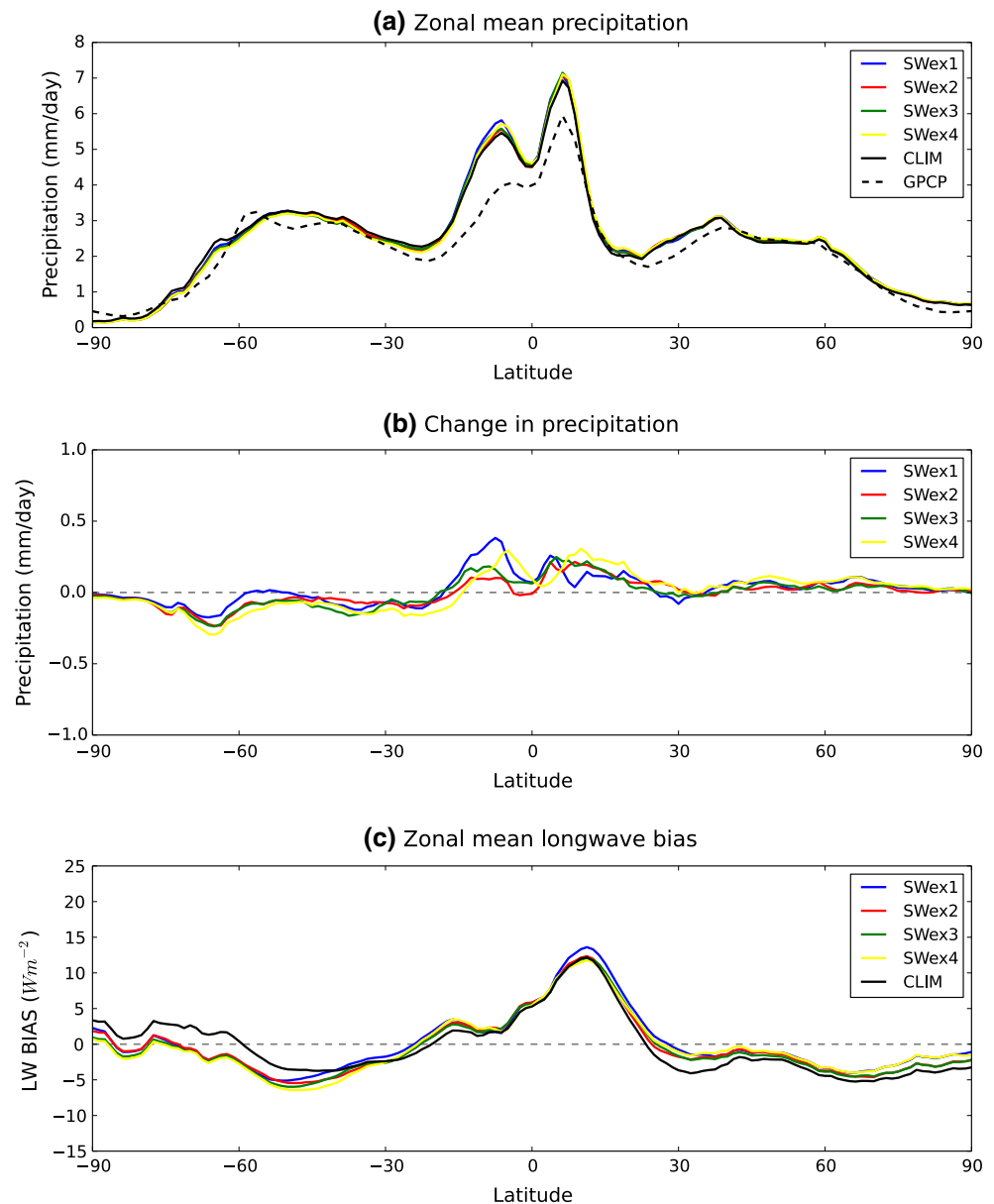


Fig. 3 Zonal mean eastward wind (**a** m s^{-1}) and precipitation (**f** mm day^{-1}) in the CLIM simulation and the difference in eastward wind (**b–e**) and precipitation (**g–j**) between the four SWex experiments and the CLIM simulation

extratropics, the increase is largely achieved in the atmosphere. Resultantly, improvements in TET in the tropics do not lead to improvements in the representation of the ITCZ as the tropical/cross-equatorial AET—which has frequently been cited in the literature as a key determinant of the ITCZ location (see, for example, Voigt et al. 2014a, b)—does not materially improve (see Fig. 6a and inset). The cross-equatorial OET, in contrast, is more closely comparable to observations in the SWex simulations than CLIM. In Haywood et al. (2016) the cross-equatorial transport in the atmosphere exhibited more significant improvement, with the northward AET bias from the model climatology reversed in all experiments (see their Figure 3a).

The partitioning of the energy transport adjustments between atmosphere/ocean in the tropics/extratropics (Fig. 6b) bear remarkable similarity to those of Kay et al. (2016), using a different model and experimental design to impose similar perturbations to the TOA energy budget in the CESM-CAM5 model in the tropics and extratropics. Kay et al. (2016) also found a tropical response dominated by ocean responses in the Pacific and extratropical TET adjustments in the Southern Hemisphere dominated by the atmospheric response. An experiment run with only the extratropical albedo forcing in both hemispheres and no tropical perturbation (not shown) has a similar extratropical response, with a strengthening of the jet and increase in AET in the mid-latitudes, and little change in

Fig. 4 Zonal mean **a** precipitation in CLIM and SWex compared to GPCP (mm day^{-1}), **b** change in precipitation from CLIM to SWex and **c** TOA outgoing longwave radiation bias in CLIM and SWex compared to CERES (W m^{-2} , upwards as positive)



cross-equatorial AET. Given the TOA energy budget is not in balance in such an experiment the climate system and cross-equatorial energy transport begins to adjust after several years to the net cooling forced from the Southern Hemisphere, though the AET response remains muted through the tropics in the first two decades.

Further insight into the response is gained by examining the contribution to changes in OET of each ocean basin (Fig. 7). It is apparent that almost all of the global OET adjustments occur in the Pacific, a result consistent with the largest precipitation changes being in the Pacific (see Fig. 3g–j). Qualitatively, the adjustments in TET, AET and OET occur in the first few years of the experiments (not shown), indicating that the ocean is being driven by changes in atmospheric circulation, rather than deep ocean

processes governing the overall response of the model. Mean zonal wind increases associated with an acceleration of the jet (Fig. 3b–e) have differential meridional teleconnections (Fig. 8a–b), with the most significant sub-tropical and tropical teleconnections occurring in the Pacific. The dynamical response in all SWex experiments is qualitatively similar, so only one ensemble member is shown here.

Increased convergence around the SPCZ, forced from both the extratropics and a strengthening of the subtropical anticyclone in the south-east Pacific, is associated with increased precipitation and an extension of the SPCZ (Fig. 8b). The intensified midlatitude zonal winds (Fig. 3b–e) increase surface wind stress (not shown) and upper ocean divergence, centred on the location of maximum wind stress, around 58°S, increases slightly in response to this

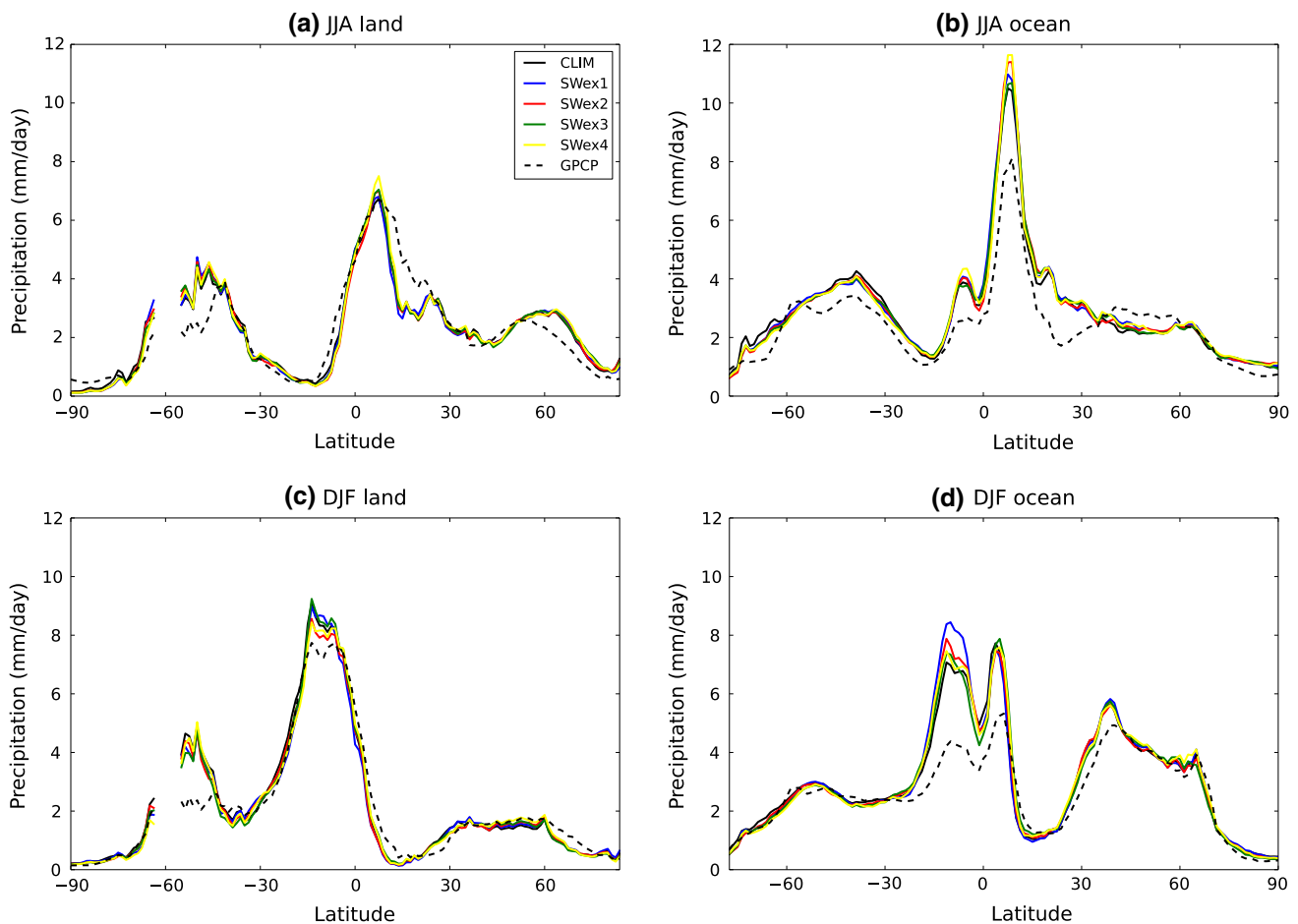


Fig. 5 Zonal mean precipitation in CLIM and SWex compared to GPCP (mm day^{-1}) in JJA (**a**, **b**) and DJF (**c**, **d**) over land (**a**, **c**) and ocean (**b**, **d**) points

forcing (Fig. 8d). Changes in OET are minor at these latitudes (Fig. 6). In the tropics, where the OET response dominates the TET changes, the increased southward energy transport appears to be primarily driven by increased energy flux into the ocean and increased SSTs (Fig. 8e–f), related to the increase in absorbed shortwave radiation induced by the reduction in albedo. The Southern Hemisphere branch of the Pacific tropical cells (see e.g. Johnson et al. 2001; Perez and Kessler 2009) in the upper ocean (Fig. 8c–d) respond to wind stress anomalies related to the SPCZ intensification, though the changes in mass transport are minor relative to the overall intensity of the cells such that the increased energy content of the upper ocean, reflected by the SST increases, dominates the response. In the Northern Hemisphere, a reduction in the intensity of the Pacific tropical cells leads to reductions in the northward OET near the equator. Further north, the changes in circulation patterns are muted, reflective of the fact the model response is primarily manifested in the Southern Hemisphere and southern branch of the Hadley cell.

These experiments show that dynamical responses are sensitive to the formulation of the model simulation. Perturbing hemispheric albedo properties (or otherwise inducing cross-equatorial energy transport changes) in simplistic frameworks may induce a response in the climate system associated with experimental design, rather than dynamical responses which can be considered in relation to our understanding of the observed climate system. Though these results may also partly be a function of experimental design, we note the consistency of response in the Haywood et al. (2016) experiments to stratospheric, ocean and cloud forcing and also the similarity of these results to those of Kay et al. (2016), where perturbations to the energy budget were applied via altering cloud parameterisations. In the SWex simulations, little reduction in zonal mean longwave biases is achieved (Fig. 4b), which can be related to the only partial improvement in TET (Fig. 6). We therefore proceed by reducing tropical longwave biases to examine the dynamical response to improving both TOA longwave

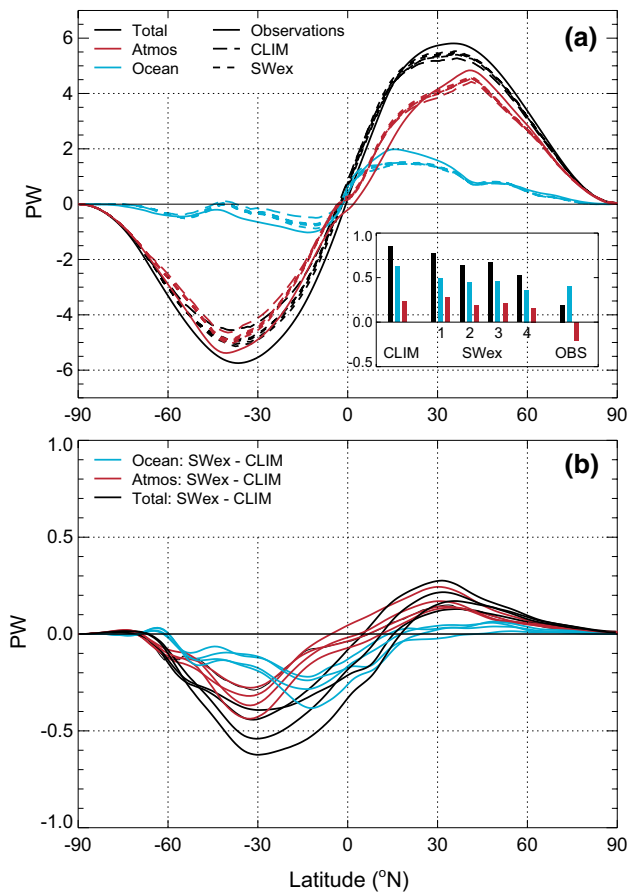


Fig. 6 Annual mean meridional energy transport: **a** total (black), ocean (blue) and atmospheric (red) components of the energy transport (PW, northward positive) in observations (solid), CLIM (long dashes) and the four SWEx experiments (dashed), **b** the difference in the total/ocean/atmosphere between CLIM and the SWEx experiments. The bar plot embedded within **a** shows the cross-equatorial energy transport (PW, northward positive) with colours as for the other plots

and shortwave biases and thus ‘forcing’ TET further towards observed values.

3.2 Shortwave and longwave bias reduction

In Fig. 9 the TOA SW, LW and total radiation biases are shown in the CLIM experiment and for the SWLWex simulations. In these experiments, the ocean albedo forcing from SWEx2 and SWEx3 (the two intermediate experiments) is combined with a perturbation to the cloud climatology in the tropics, as described in Sect. 2.2. The tropical clouds are only active in the longwave and are inserted between 10°S and 30°N with varying optical depth to target the magnitude of the TOA LW bias at each latitude. Figure 9b shows the reduction in outgoing LW in the tropics which this achieves, with a small adjustment in outgoing SW (Fig. 9a) when compared to the SWEx simulations

(see Fig. 2b) associated with changes in cloud cover. Biases in the total TOA radiation budget (Fig. 9c) at almost all latitudes, particularly the areas of the tropics and southern hemisphere extratropics where the main biases in CLIM are situated, are reduced and the changes in the total TOA bias are greater than in the SWEx simulations (see Fig. 2d).

As a result of these changes in the TOA energy budget of the model, more energy is exported from the tropics. Figure 10 shows the meridional energy transport, as in Fig. 6. In both hemispheres, the changes in TET from the SWEx ensemble are primarily a function of increased poleward energy transport in the atmosphere (Fig. 10b). Cross-equatorial energy transport in the atmosphere improves (Fig. 10a, inset) and there is a general improvement in meridional energy transport with respect to observations across the Southern Hemisphere. The general increase in AET in the Northern Hemisphere represents an improvement in the mid-latitudes though not the tropics. The comparability of TET in SWLWex and observations between 0 and 30°N is a function of error compensations between OET and AET. In the Southern Hemisphere tropics, increases in poleward AET occur though do not reduce the TET biases dramatically. However, changes in zonal mean precipitation biases—annually, seasonally and when subdivided between ocean and land (as in Fig. 5)—are small relative to the magnitude of the biases in the CLIM and SWEx experiments (not shown).

Synthesising these results, forcing the TOA energy budget towards observations, via both shortwave (SWEx) and shortwave+longwave (SWLWex) adjustments, has not provided a material improvement in the representation of tropical precipitation. The greater improvement in the cross-equatorial atmospheric energy transport in the SWLWex ensemble is not reflective of a broader improvement in meridional energy transport and atmospheric circulation. This metric might justifiably be considered a useful first order constraint on climate model fidelity, as an index of the southern branch of the Hadley circulation. However, the approach used here has not sought to improve the underlying physical biases in the model which cause deficiencies in the model climatology. Cloud biases in both the extratropics and tropics are associated with the TOA energy budget biases. An evaluation of the dry and moist components of the AET shows that the partitioning of the atmospheric meridional energy transport between latent and dry energy does not compare well to reanalysis (Fig. 11). In the tropics, the partitioning of energy transport within the Hadley cell is observed as dry energy moving away from the ITCZ and latent energy converging towards the ITCZ. Biases in both components balance out to provide a reasonable representation of total atmospheric energy transport which masks these deficiencies. Beyond 25°S–25°N the partitioning between model and reanalysis is starkly divergent,

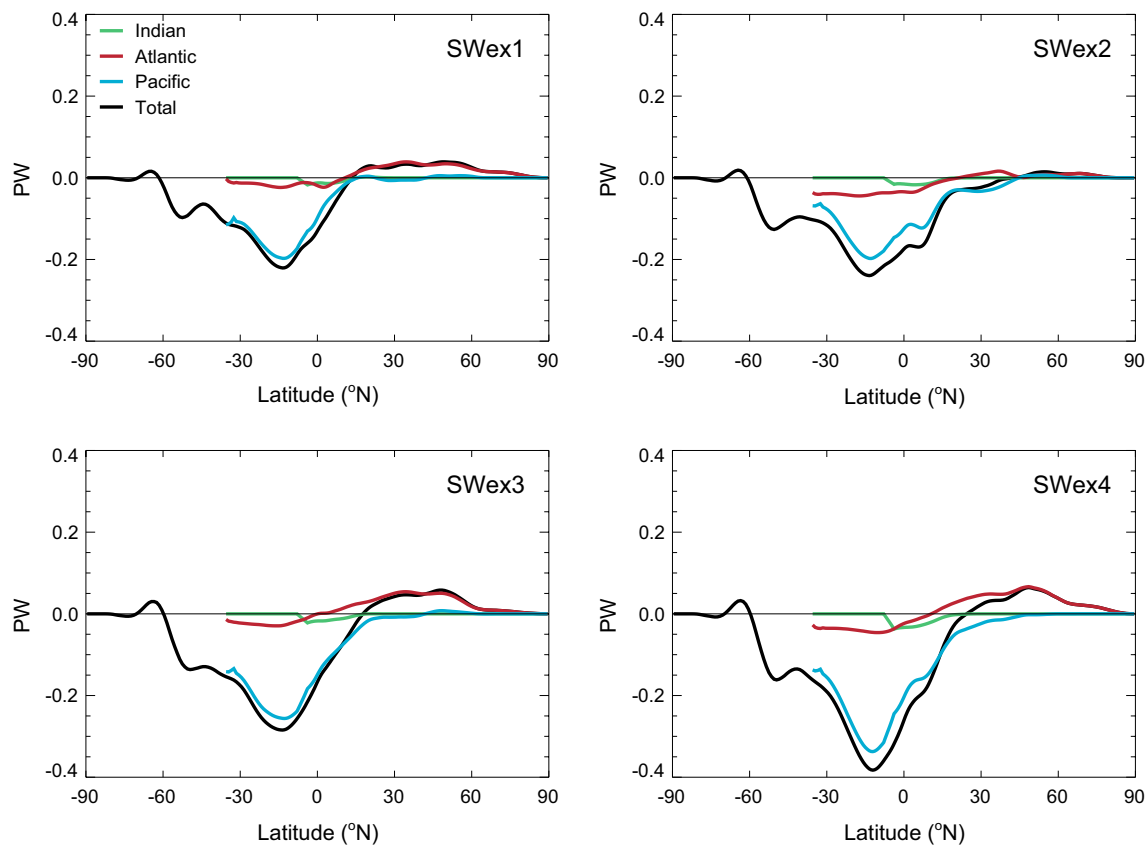


Fig. 7 Change in annual mean meridional energy transport (PW, northward *positive*) from the CLIM simulation for total ocean energy transport (*black*), Pacific (*blue*), Atlantic (*red*) and Indian (*green*) Oceans. In the model, Indian Ocean fluxes are only output to 5°S.

with too little dry energy transport into the extratropics in the model compensated by excessive latent energy transport. This partitioning in the atmospheric energy transport is again reflective of biases in the representation of physical processes in the model and it is these processes which influence the biases in cloud cover and energy transport observed in HadGEM2-ES and other climate models. Metrics which relate biases in the extratropics to the ITCZ and cross-equatorial energy transport are useful for model evaluation, though without understanding the sources and nature of the biases in physical processes which control those relationships in individual models they do not provide a route for model improvement.

4 Conclusions

The primary focus of this study has been to investigate the tropical response to a cooling of the Southern Hemisphere extratropics and adjustment of inter-hemispheric albedo within the coupled model framework. We increase

The southern Indian Ocean fluxes are included in the Pacific transport term, though are small relative to the total energy transport in the Pacific basin

albedo in the Southern Ocean to mimic the energy budget impact that would occur if cloud biases in this region were reduced. We further reduce albedo in the tropics to balance global TOA energy budgets and also reduce albedo biases in the model climate in this region. The net effect of these changes is to change the meridional (and cross-equatorial) energy transport in the model, HadGEM2-ES, which has both Southern Ocean and tropical cloud biases typical of the current generation of climate models (see Bodas-Salcedo et al. 2014; Li et al. 2013).

The main findings of this study are as follows:

- Perturbing inter-hemispheric albedo through targeted corrections to model TOA radiation biases does not yield significant improvement to the representation of the climate of the tropics.
- Changes in cross-equatorial energy transport are largely in the ocean, which mutes the atmospheric response. In a slab ocean framework, the response would be limited to the atmosphere, which may result in significant improvements to the tropical climate.

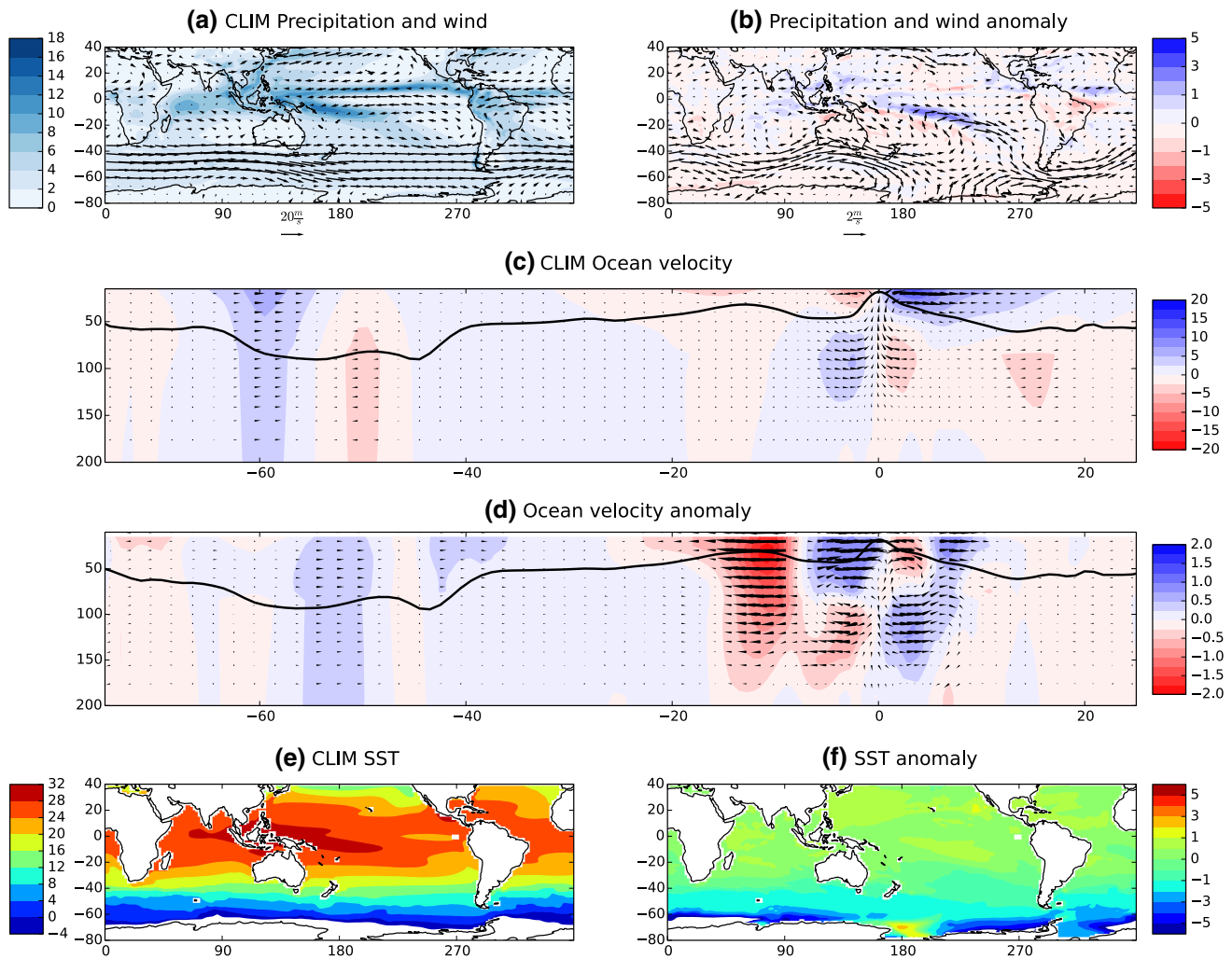


Fig. 8 Precipitation (**a** mm day^{-1}) and mean 1000–500 hPa wind (**a** m s^{-1}), transect of ocean circulation averaged between 190 and 210E showing meridional velocities (*coloured contours* cm s^{-1}), normalised circulation vectors and thermocline depth (*line contour*) (**c**) and

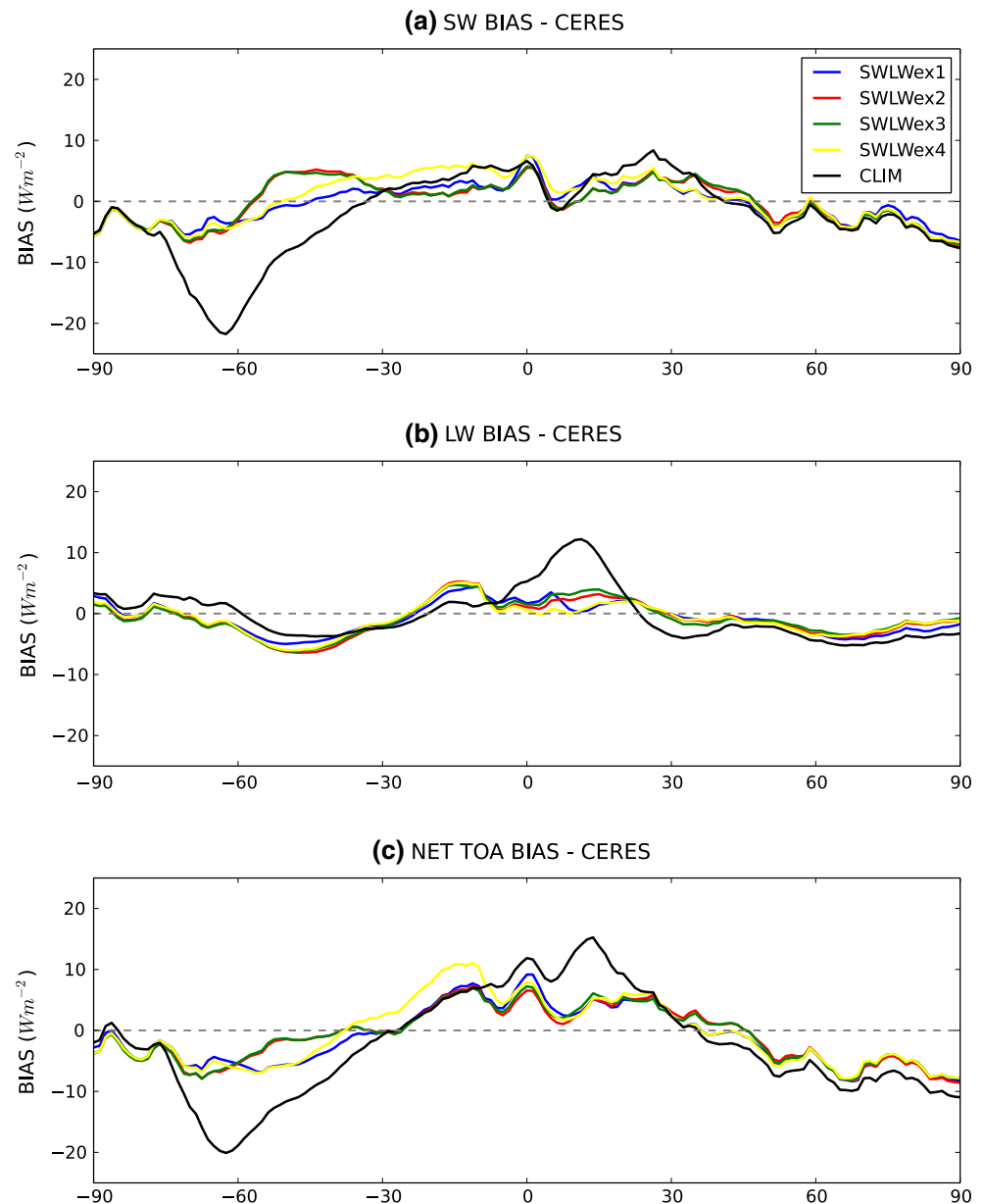
SSTs (**e**), $^{\circ}\text{C}$) in the CLIM simulation and the difference between the SWex3 experiment and CLIM simulation (**b**, **d**, **f**) for those fields. In **d** the vectors are scaled as for the colour contours—a 1:10 ratio of the length in **c**—and the absolute thermocline depth is shown for SWex3

- Cross-equatorial energy transport is an important index of model fidelity, but the correct partitioning between atmosphere and ocean is key to improving the representation of the tropics.
- Model response is dependent on the nature of the forcing applied—simplified, hemisphere wide corrections to albedo may yield very different results to latitudinally varying forcings.
- Simplified corrections to TOA radiation biases do not attend to the underlying biases in physical processes which appear to drive biases in energy transport, limiting the improvement in model climate which may be achieved in such experiments.

Several studies have noted changes in the ITCZ occur as cross-equatorial energy transport responds to

differential albedo or net energy balance in the two hemispheres, though these studies have largely been undertaken without a dynamical ocean (e.g. Kang et al. 2008; Frierson and Hwang 2012; Cvijanovic and Chiang 2013; Voigt et al. 2014b). In this study, the use of a coupled ocean leads to the tropical and cross-equatorial energy transport changes being partitioned such that the majority of the response is in the ocean. As a result, no improvement is seen in the representation of the tropical atmosphere. The double ITCZ bias in the model persists and cross-equatorial atmospheric energy transport biases are not reduced in experiments where the albedo is adjusted. In contrast, the jet in the southern hemisphere strengthens with increases in atmospheric energy transport related to the increase in temperature gradient into the extratropics.

Fig. 9 Top of atmosphere net shortwave (a), longwave (b) and total net radiation (c) W m^{-2} , upwards as *positive* zonal mean biases in CLIM and the SWLWex experiments compared to CERES



The study of Haywood et al. (2016) corrected the gross bias in the hemispheric albedo, though the improvements in tropical performance in that study appear to be linked to the improved representation of cross-equatorial energy transport, which is intrinsically linked to moisture transport via the Hadley circulation (Frierson et al. 2013). These improvements may be related to the induction of a strong tropical SST gradient anomaly and local improvements in cross-equatorial atmospheric heat transport, which are not reflective of wider improvements in the model climate. The more refined treatment of albedo correction applied in the current study reveals little improvement in cross-equatorial atmospheric heat transport and therefore little improvement in tropical precipitation.

These results are remarkably similar to those of Kay et al. (2016), where reductions in Southern Ocean cloud biases induce similar changes in meridional energy transport. It is notable that the two studies yield analogous results from forcing two independent atmosphere and ocean models with perturbations at the ocean surface (this study) and through altering cloud parameterisations (Kay et al.), suggesting these results may not be model specific. In addition to supporting the results and conclusions of Kay et al., further experiments performed in this study which investigate the impact of reducing tropical LW biases do not yield improvements in model performance. The recent study of Deser et al. (2015) further emphasises the differential global climate response that may be observed in

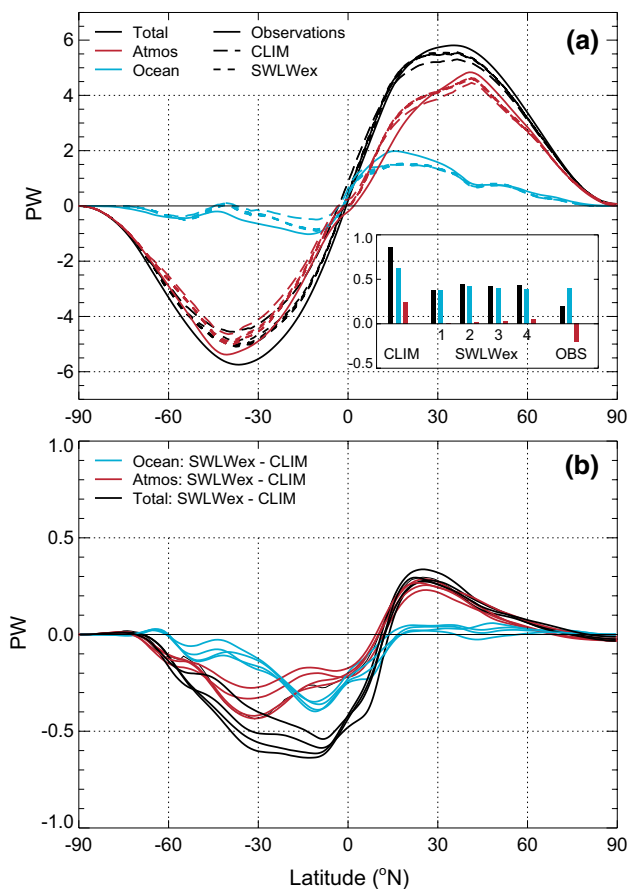


Fig. 10 Annual mean meridional energy transport: **a** total (black), ocean (blue) and atmospheric (red) components of the energy transport (PW, northward positive) in observations (solid), CLIM (long dashes) and the four SWLWex experiments (dashed), **b** the difference in the total/ocean/atmosphere between CLIM and the SWLWex experiments. The bar plot embedded within **a** shows the cross-equatorial energy transport (PW, northward positive) with colours as for the other plots

coupled and slab ocean experiments when the extratropics are perturbed. To consider global teleconnections of regional changes in model climate, considering the atmosphere in isolation may be insufficient if the results are to be interpreted with respect to the observed climate system.

A further ensemble of experiments which reduce biases in both the global TOA shortwave (via ocean albedo modification) and tropical TOA longwave (via inserting an additional cirrus-like cloud climatology) to force the model’s energy transport towards observations do not yield significant further improvement in the model climate. The underlying physical biases in the model, such as moist processes in the atmosphere, are not changed through the simple forcings applied here. Donohoe and Battisti (2012) have previously noted that the spread in maximum meridional heat transport in the CMIP3 models is primarily a function of cloud properties. Hwang and Frierson (2013)

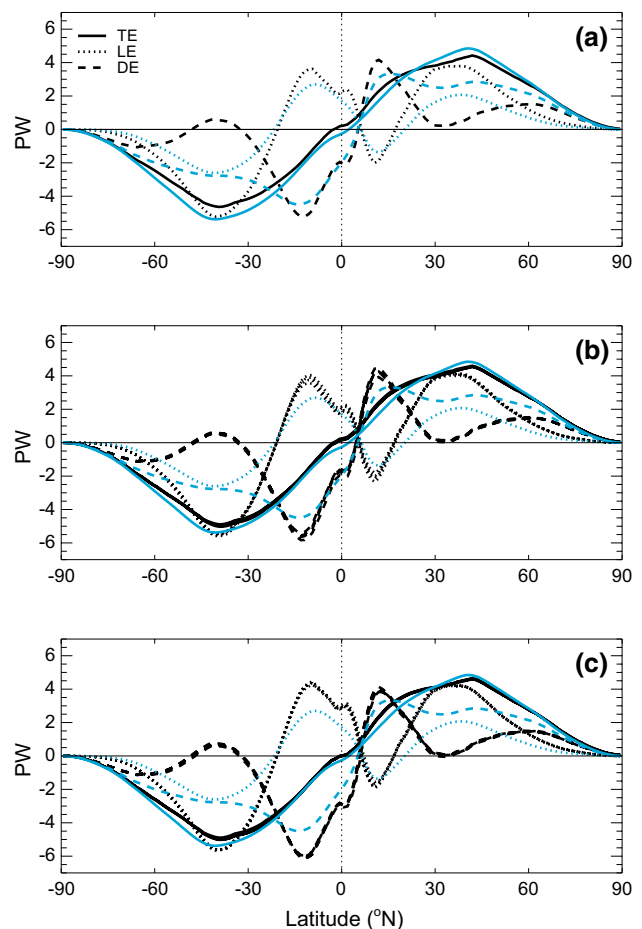


Fig. 11 Annual mean meridional energy transport (PW) in the atmosphere in HadGEM2-ES (black) and ERAI (blue) for **a** the CLIM simulation, **b** the SWex experiments and **c** the LWSWex experiments. The total AET (TE, solid lines), latent energy (LE, dotted lines) and dry energy (DE, dashed lines) transport terms are shown

have shown that the spread in Southern Ocean cloud biases in the CMIP5 models explains much of the difference in southern hemisphere tropical precipitation biases in those models. The impact of these biases may not easily be constrained by blunt instruments which target the TOA energy budgets.

Though the results of this work are limited to a single model, the study investigates the impact of reducing a long standing extratropical climate model bias and, perhaps contrary to expectations, does not yield improvements in the tropical climate. Simplified corrections which do not correct the underlying biases in the physical processes, such as convective-dynamical coupling in the tropics, are unable to yield substantial improvements in the representation of the tropics. The use of a dynamical ocean appears key to understanding the full model response to inter-hemispheric climate perturbations—without a coupled ocean the climate response can only occur in the atmosphere,

such that observed improvements in model performance may well be a case of getting the right result for the wrong reasons.

Acknowledgments M.K.H., M.C. and J.M.H. were supported by the Natural Environment Research Council/Department for International Development via the Future Climates for Africa (FCFA) funded project 'Improving Model Processes for African Climate' (IMPALA, NE/M017265/1). J.M.H. and A.J. were supported by the Joint UK DECC/Defra Met Office Hadley Centre Climate Programme (GA01101). The authors thank the editor and two anonymous reviewers for constructive and insightful comments that helped improve the manuscript.

Open Access This article is distributed under the terms of the Creative Commons Attribution 4.0 International License (<http://creativecommons.org/licenses/by/4.0/>), which permits unrestricted use, distribution, and reproduction in any medium, provided you give appropriate credit to the original author(s) and the source, provide a link to the Creative Commons license, and indicate if changes were made.

References

- Adler RF, Huffman GJ, Chang A, Ferraro R, Xie PP, Janowiak J, Rudolf B, Schneider U, Curtis S, Bolvin D et al (2003) The version-2 global precipitation climatology project (GPCP) monthly precipitation analysis (1979–present). *J Hydrometeorol* 4(6):1147–1167
- Adler RF, Gu G, Huffman GJ (2012) Estimating climatological bias errors for the global precipitation climatology project (GPCP). *J Appl Meteorol Climatol* 51(1):84–99
- Balmaseda MA, Mogensen K, Weaver AT (2013) Evaluation of the ECMWF ocean reanalysis system ORAS4. *Q J R Meteorol Soc* 139(674):1132–1161
- Bodas-Salcedo A, Williams K, Field P, Lock A (2012) The surface downwelling solar radiation surplus over the southern ocean in the met office model: the role of midlatitude cyclone clouds. *J Clim* 25(21):7467–7486
- Bodas-Salcedo A, Williams KD, Ringer MA, Beau I, Cole JN, Dufresne JL, Koshiro T, Stevens B, Wang Z, Yokohata T (2014) Origins of the solar radiation biases over the Southern Ocean in CFMIP2 models*. *J Clim* 27(1):41–56
- Chiang JC, Bitz CM (2005) Influence of high latitude ice cover on the marine intertropical convergence zone. *Clim Dyn* 25(5):477–496
- Collins W, Bellouin N, Doutriaux-Boucher M, Gedney N, Halloran P, Hinton T, Hughes J, Jones C, Joshi M, Liddicoat S et al (2011) Development and evaluation of an earth-system model–HadGEM2. *Geosci Model Dev* 4(4):1051–1075
- Cvijanovic I, Chiang JC (2013) Global energy budget changes to high latitude North Atlantic cooling and the tropical ITCZ response. *Clim Dyn* 40(5–6):1435–1452
- Dai A (2006) Precipitation characteristics in eighteen coupled climate models. *J Clim* 19(18):4605–4630
- Dee D, Uppala S, Simmons A, Berrisford P, Poli P, Kobayashi S, Andrae U, Balmaseda M, Balsamo G, Bauer P et al (2011) The ERA-interim reanalysis: configuration and performance of the data assimilation system. *Q J R Meteorol Soc* 137(656):553–597
- Deser C, Tomas RA, Sun L (2015) The role of ocean–atmosphere coupling in the zonal-mean atmospheric response to Arctic sea ice loss. *J Clim* 28(6):2168–2186
- Doelling DR, Loeb NG, Keyes DF, Nordeen ML, Morstad D, Nguyen C, Wielicki BA, Young DF, Sun M (2013) Geostationary enhanced temporal interpolation for CERES flux products. *J Atmos Ocean Technol* 30(6):1072–1090
- Donohoe A, Battisti DS (2012) What determines meridional heat transport in climate models? *J Clim* 25(11):3832–3850
- Frierson DM, Hwang YT (2012) Extratropical influence on ITCZ shifts in slab ocean simulations of global warming. *J Clim* 25(2):720–733
- Frierson DM, Hwang YT, Fučkar NS, Seager R, Kang SM, Donohoe A, Maroon EA, Liu X, Battisti DS (2013) Contribution of ocean overturning circulation to tropical rainfall peak in the northern hemisphere. *Nat Geosci* 6(11):940–944
- Haywood JM, Jones A, Bellouin N, Stephenson D (2013) Asymmetric forcing from stratospheric aerosols impacts Sahelian rainfall. *Nat Clim Change* 3(7):660–665
- Haywood JM, Jones A, Dunstone N, Milton S, Vellinga M, Bodas-Salcedo A, Hawcroft M, Kravitz B, Cole J, Watanabe S et al (2016) The impact of equilibrating hemispheric albedos on tropical performance in the HadGEM2-ES coupled climate model. *Geophys Res Lett* 43:395–403
- Heuzé C, Heywood KJ, Stevens DP, Ridley JK (2013) Southern Ocean bottom water characteristics in CMIP5 models. *Geophys Res Lett* 40(7):1409–1414
- Hwang YT, Frierson DM (2013) Link between the double-intertropical convergence zone problem and cloud biases over the southern ocean. *Proc Nat Acad Sci* 110(13):4935–4940
- Jiang JH, Su H, Zhai C, Perun VS, Del Genio A, Nazarenko LS, Donner LJ, Horowitz L, Seman C, Cole J et al (2012) Evaluation of cloud and water vapor simulations in CMIP5 climate models using NASA A-train satellite observations. *J Geophys Res Atmos* 117(D14). doi:10.1029/2011JD017237
- Johnson GC, McPhaden MJ, Firing E (2001) Equatorial Pacific ocean horizontal velocity, divergence, and upwelling*. *J Phys Oceanogr* 31(3):839–849
- Kang SM, Held IM, Frierson DM, Zhao M (2008) The response of the ITCZ to extratropical thermal forcing: idealized slab-ocean experiments with a GCM. *J Clim* 21(14):3521–3532
- Kato S, Loeb NG, Rose FG, Doelling DR, Rutan DA, Caldwell TE, Yu L, Weller RA (2013) Surface irradiances consistent with CERES-derived top-of-atmosphere shortwave and longwave irradiances. *J Clim* 26(9):2719–2740
- Kay JE, Wall C, Yettella V, Medeiros B, Hannay C, Caldwell P, Bitz C (2016) Global climate impacts of fixing the Southern Ocean shortwave radiation bias in the community earth system model (CESM). *J Clim*. doi:10.1175/JCLI-D-15-0358.1
- Li JL, Waliser D, Stephens G, Lee S, L'Ecuyer T, Kato S, Loeb N, Ma HY (2013) Characterizing and understanding radiation budget biases in CMIP3/CMIP5 GCMs, contemporary GCM, and reanalysis. *J Geophys Res Atmos* 118(15):8166–8184
- Loeb NG, Wielicki BA, Doelling DR, Smith GL, Keyes DF, Kato S, Manalo-Smith N, Wong T (2009) Toward optimal closure of the Earth's top-of-atmosphere radiation budget. *J Clim* 22(3):748–766
- Loeb NG, Kato S, Su W, Wong T, Rose FG, Doelling DR, Norris JR, Huang X (2012a) Advances in understanding top-of-atmosphere radiation variability from satellite observations. *Surv Geophys* 33(3–4):359–385
- Loeb NG, Lyman JM, Johnson GC, Allan RP, Doelling DR, Wong T, Soden BJ, Stephens GL (2012b) Observed changes in top-of-the-atmosphere radiation and upper-ocean heating consistent within uncertainty. *Nat Geosci* 5(2):110–113
- Loeb NG, Wang H, Cheng A, Kato S, Fasullo JT, Xu KM, Allan RP (2015) Observational constraints on atmospheric and oceanic cross-equatorial heat transports: revisiting the precipitation asymmetry problem in climate models. *Clim Dyn* 46:3239–3257
- Meijers A (2014) The Southern Ocean in the coupled model inter-comparison project phase 5. *Philos Trans R Soc Lond A Math Phys Eng Sci* 372(2019):20130,296

- Menary MB, Scaife AA (2014) Naturally forced multidecadal variability of the Atlantic meridional overturning circulation. *Clim Dyn* 42(5–6):1347–1362
- Menary MB, Roberts CD, Palmer MD, Halloran PR, Jackson L, Wood RA, Mueller WA, Matei D, Lee SK (2013) Mechanisms of aerosol-forced AMOC variability in a state of the art climate model. *J Geophys Res Oceans* 118(4):2087–2096
- NCAR (2014) National center for atmospheric research staff (eds). The climate data guide: era-interim: derived components. <https://climatedataguide.ucar.edu/climate-data/era-interim-derived-components>. Accessed 2015-02-12
- Palmer M, Roberts C, Balmaseda M, Chang YS, Chepurin G, Ferry N, Fujii Y, Good S, Guinehut S, Haines K et al (2015) Ocean heat content variability and change in an ensemble of ocean reanalyses. *Clim Dyn*. doi:10.1007/s00382-015-2801-0
- Perez RC, Kessler WS (2009) Three-dimensional structure of tropical cells in the central equatorial Pacific Ocean. *J Phys Oceanogr* 39(1):27–49
- Stephens GL, L'Ecuyer T (2015) The Earth's energy balance. *Atmos Res* 166:195–203
- Stephens GL, Hakuba MZ, Hawcroft MK, Haywood JM, Behrangi A, Kay JE, Webster PJ (2016) The curious nature of the hemispheric symmetry of the Earth's water and energy balances. *Curr Clim Chang Rep* (in revision)
- Taylor KE, Stouffer RJ, Meehl GA (2012) An overview of CMIP5 and the experiment design. *Bull Am Meteorol Soc* 93(4):485–498
- Van Der Wiel K, Matthews AJ, Joshi MM, Stevens DP (2015a) Why the South Pacific convergence zone is diagonal. *Clim Dyn* 46(5):1683–1698
- Van Der Wiel K, Matthews AJ, Stevens DP, Joshi MM (2015b) A dynamical framework for the origin of the diagonal South Pacific and South Atlantic Convergence Zones. *Q J R Meteorol Soc* 141(691):1997–2010
- Voigt A, Bony S, Dufresne JL, Stevens B (2014a) The radiative impact of clouds on the shift of the intertropical convergence zone. *Geophys Res Lett* 41(12):4308–4315
- Voigt A, Stevens B, Bader J, Mauritsen T (2014b) Compensation of hemispheric albedo asymmetries by shifts of the ITCZ and tropical clouds. *J Clim* 27(3):1029–1045
- Wielicki BA, Barkstrom BR, Harrison EF, Lee RB III, Louis Smith G, Cooper JE (1996) Clouds and the Earth's Radiant Energy System (CERES): an earth observing system experiment. *Bull Am Meteorol Soc* 77(5):853–868
- Williams K, Bodas-Salcedo A, Déqué M, Fermepin S, Medeiros B, Watanabe M, Jakob C, Klein S, Senior C, Williamson D (2013) The transpose-AMIP II experiment and its application to the understanding of Southern Ocean cloud biases in climate models. *J Clim* 26(10):3258–3274
- Zhang X, Liu H, Zhang M (2015) Double ITCZ in coupled ocean-atmosphere models: from CMIP3 to CMIP5. *Geophys Res Lett* 42(20):8651–8659